



A case-study analysis of surface/upper-air coupling in southeastern Montana
by Orville Dennis Green

A thesis submitted in partial fulfillment of the requirements for the degree of Master of Science in
Earth Science

Montana State University

© Copyright by Orville Dennis Green (1986)

Abstract:

Rawinsonde data collected during the Cooperative Convective Precipitation Experiment (CCOPE) were analyzed to search for evidence of surface/upper-air coupling in southeastern Montana. CCOPE, an outgrowth of the HIPLEX-I weather modification project, was conducted near the semi-arid region of Miles City, Montana, during the summer of 1981. Five raw insonde stations were used in a limited station analysis scheme to examine three periods possessing varying degrees of convection.

The case-studies covered a severe-storm period (June 12-13), which produced radar reflectivities in excess of 50 dBz and a relatively large amount of precipitation; an intermediate convective period (June 20-21) characterized by the occurrence of small, semi-isolated cumuli selected as experimental units for the HIPLEX-I weather modification experiment; and a convectively benign period (July 30-31) with little or no visible convection. Surface/upper-air coupling during these periods was investigated by comparing vertical plots of areally averaged primary and derived meteorological parameters with corresponding temporal surface patterns.

Results suggest that surface/upper-air coupling, manifest as downward-propagating sinusoidal convergence and vorticity patterns, is more clearly established during the severe-storm period, evident to a lesser degree during the intermediate convective period, and absent during the benign period. Analogous analyses using nearby surface stations indicate that these patterns are reflected on the surface. However, the strongest evidence of surface/upper-air coupling based on surface information alone appears to be surface convergence and relative vorticity couplets of like sign.

Other features of the severe-storm period include a low-level jet with significant moisture advection, and an unstable total specific atmospheric energy profile aloft. These features were less striking or absent on the other case-study days.

A CASE-STUDY ANALYSIS OF SURFACE/UPPER-AIR COUPLING
IN SOUTHEASTERN MONTANA

by

Orville Dennis Green

A thesis submitted in partial fulfillment
of the requirements for the degree

of

Master of Science

in

Earth Science

MONTANA STATE UNIVERSITY
Bozeman, Montana

June 1986

APPROVAL

of a thesis submitted by

Orville Dennis Green

This thesis has been read by each member of the thesis committee and has been found to be satisfactory regarding content, English usage, format, citations, bibliographic style, and consistency, and is ready for submission to the College of Graduate Studies.

20 May 1986

Date

James A. Kernbach, Jr.

Chairperson, Graduate Committee

Approved for the Major Department

20 May 86

Date

Joseph A. A.

Head, Major Department

Approved for the College of Graduate Studies

June 11, 1986

Date

Henry S. Parsons

Graduate Dean

STATEMENT OF PERMISSION TO USE

In presenting this thesis in partial fulfillment of the requirements for a master's degree at Montana State University, I agree that the Library shall make it available to borrowers under rules of the Library. Brief quotations from this thesis are allowable without special permission, provided that accurate acknowledgment of source is made.

Permission for extensive quotation from or reproduction of this thesis may be granted by my major professor, or in his absence, by the Director of Libraries when, in the opinion of either, the proposed use of the material is for scholarly purposes. Any copying or use of the material in this thesis for financial gain shall not be allowed without my written permission.

Signature Orville Green

Date May 19, 1986

ACKNOWLEDGEMENT

For the many hours of patient encouragement and direction, I express my grateful appreciation to Dr. James A. Heimbach, Jr. I am also grateful for the contributions of Dr. Steve Custer, Dr. Joe Ashley, and Dr. Kathy Hansen-Bristow, who provided several useful comments during their critical review of this thesis. Mrs. Ann Parker was of considerable help in the preparation of the final copy of this manuscript.

This research was funded by the Experimental Meteorology Branch, National Science Foundation, Grant ATM-8209836.

TABLE OF CONTENTS

	Page
1. INTRODUCTION	1
Upper-Air Measurements	1
The Cooperative Convective Precipitation Experiment.	2
Focus of Current Study	4
Thesis Statement	5
2. HISTORICAL BACKGROUND.	6
The Thunderstorm Project	6
Relevant Surface Research.	8
Relevant Upper-Air Research.	10
Relevant Research in Southeastern Montana.	11
3. DATABASE DESCRIPTION	12
4. PROCEDURES	16
Sequence of Operations	16
Data Adjustments	19
Interpolation.	19
Balloon Drift.	20
Surface/Upper-Air Comparisons.	20
Network Differences.	20
Coordinate Reference Frames.	21
Data Processing Methods.	22
Evaluation of Meteorological Parameters.	22
Vapor Pressure	22
Absolute Humidity.	23
Specific Humidity.	23
Mixing Ratio	23
Relative Humidity.	23
Virtual Temperature.	24
Potential Temperature.	24
Equivalent Temperature	24
Equivalent Potential Temperature	24
Total Specific Atmospheric Energy.	25
Horizontal Kinematic Convergence	25
Vertical Component of the Relative Vorticity Vector.	25
Horizontal Moisture Convergence.	26
Vertical Velocity.	26

TABLE OF CONTENTS--Continued

	Page
5. CASE-STUDY ANALYSES.	27
Case-Study : The Severe-storm Period (12-13 June 1981)	29
General Meteorological Conditions During Severe-storm Case	29
Surface Patterns During the Severe-storm Case.	32
Surface Indications Prior to Precipitation Event #1.	34
Surface Indications During Precipitation Event #1.	34
Surface Indications During Precipitation Event #2.	38
Surface Indications During Precipitation Event #3.	38
Summary of Major Surface Features During Severe-storm Case	39
Upper-Air Profiles During the Severe-storm Case.	39
Surface/Upper-Air Coupling During the Severe-storm Case.	52
Case-Study : The HIPLEX-I Period (20-21 June 1981)	58
General Meteorological Conditions During the HIPLEX-I Case	58
Surface Patterns During the HIPLEX-I Case.	58
Upper-Air Profiles During the HIPLEX-I Case.	61
Surface/Upper-Air Coupling During the HIPLEX-I Case.	67
Case-Study : The Benign Period (30-31 July 1981)	71
General Meteorological Conditions During the Benign Case	71
Surface Patterns During the Benign Case.	71
Upper-Air Profiles During the Benign Case.	75
Surface/Upper-Air Coupling During the Benign Case.	75
6. SUMMARY AND CONCLUSIONS.	81
REFERENCES CITED	85
APPENDICES.	90
APPENDIX A - RAWINSONDE PROGRAM LISTINGS	91
Rawinsonde mainline programs	92
RAWIN task building executive.	92
RAWIN job processing executive	94
RAWIN file interpolation module.	97
RAWIN plot module.	100
RAWIN Plot Module with Clip options.	103
Rawinsonde Subprogram Units.	108
Bubble sort.	108
File deletion.	109
Drive number	110
U,V wind components.	110
Hypsometric evaluation	111
Equivalent potential temperature	111
Equivalent temperature	112
Potential temperature.	112
Virtual temperature.	113
Relative humidity.	113

TABLE OF CONTENTS--Continued

	Page
Mixing Ratio	114
Specific humidity.	114
Vapor pressure	115
Encode an integer *1 array	116
Average RAWIN station values	117
RAWIN sounding file dump	117
Set RAWIN processing flags	119
Fetch sounding data for all required stations.	121
Get fetch list	122
Fetch sounding data.	128
Access index file.	130
Fetch module common initialization	132
RAWIN jobfile access	136
RAWIN job processing initialization.	137
Calculate MSL heights.	138
Table interpolation.	139
Input operation code	142
Set plot specification	143
Calculate abscissa parameter	144
Input abscissa parameter	149
Calculate ordinate value	150
Input ordinate parameter	152
Input station combination code	154
Encode station ids	155
Input station combinations	156
Output RAWIN table	157
Temporary communication files.	164
Set default task specifications.	165
Set task specification	166
Output task specifications	167
Read task specifications	170
Write task specifications.	172
RAWIN task building initialization	173
Directory search	181
Convert wind components into direction and speed	182
Real linear interpolation.	183
Miscellaneous FORTRAN routines	184
Miscellaneous MACRO ASSEMBLER routines	191
Rawinsonde INCLUDE Files	197
 APPENDIX B - LSA PROGRAM LISTINGS.	 203
LSA Front-end.	204
PMKIN mainline	204
Option titles.	212
Segmentation communication dummy	213
Date/time and time increment	213
Kinematic convergence.	214
Area determination	215

TABLE OF CONTENTS--Continued

	Page
Pressure change.	216
Lambert conformal projection distances	217
Vorticity.	218
Convert wind components into direction and speed	219
Average of N parameters.	219
Specific humidity and mixing ratio	220
Potential and equivalent potential temperature	220
Sea level pressure	221
Moisture convergence	221
Running means.	222
Total specific atmospheric energy.	223
LSA Intermediate Segment	224
PMKIN plot preprocessor.	224
Maximum/minimum values	229
LSA Back-end	231
PMKIN plot module.	231
APPENDIX C - PLOT PROGRAM LISTINGS	232
Plot Hardcopies.	233
Three plots per page	239
One plot per page.	252
Miscellaneous Plotting Routines.	261

LIST OF TABLES

Table	Page
1. The location and elevation of the CCOPE rawinsonde sites (BUREC, . .	14
2. Divergence calculations with and without balloon drift at the 150 mb.	20
3. Point comparisons between upper-air and surface kinematic parameters.	56

LIST OF FIGURES

Fig.	Page
1. CCOPE surface mesonet, radar, and rawinsonde sites	13
2. Procedures for construction of the rawinsonde database on the IBM PC .	18
3. Kinematic convergence using 4 stations (dashed line) and 3 stations .	28
4. Relative vorticity for the southwest quadrant (solid line) and the .	30
5. Surface and 500 mb synoptic maps at 1200 GMT on 12 June 1981, with 24.	31
6. Precipitation, specific humidity, and relative humidity for the . . .	33
7. Ambient temperature, station pressure, and total specific atmospheric.	35
8. Wind speed and wind direction for the southwest surface quadrant . . .	36
9. Kinematic convergence, moisture convergence, and relative vorticity .	37
10. Specific humidity at 2000 GMT (solid line) and 2340 GMT (dashed . . .	41
11. Relative humidity at 2000 GMT (solid line) and 2340 GMT (dashed . . .	42
12. Ambient temperature at 2000 GMT (solid line) and 2340 GMT (dashed . .	43
13. Equivalent potential temperature at 2000 GMT (solid line) and 2340 . .	44
14. Total specific atmospheric energy at 2000 GMT (solid line) and 2340 .	45
15. Wind speed at 2000 GMT (solid line) and 2340 GMT (dashed line) on 12 .	47
16. Wind direction at 2000 GMT (solid line) and 2340 GMT (dashed line) . .	48
17. Vertical velocity at 2000 GMT (solid line) and 2340 GMT (dashed . . .	49
18. Kinematic convergence at 2000 GMT (solid line) and 2340 GMT (dashed .	50
19. Moisture convergence at 2000 GMT (solid line) and 2340 GMT (dashed . .	51
20. Relative vorticity at 2000 GMT (solid line) and 2340 GMT (dashed . . .	53
21. Kinematic convergence (solid line) and relative vorticity (dashed . . .	54

LIST OF FIGURES—Continued

22. Kinematic convergence (solid line) and relative vorticity (dashed. . . 55
23. Surface and 500 mb synoptic maps at 1200 GMT on 20 June 1981, with . . 59
24. Specific humidity and relative humidity for the southwest surface. . . 60
25. Ambient temperature and total specific atmospheric energy for the. . . 62
26. Kinematic convergence, moisture convergence, and relative vorticity. . 63
27. Specific humidity at 2130 GMT (solid line) and 2344 GMT (dashed. . . . 64
28. Total specific atmospheric energy at 2130 GMT (solid line) and 2344. . 65
29. Vertical velocity at 2130 GMT (solid line) and 2344 GMT (dashed. . . . 66
30. Kinematic convergence at 2130 GMT (solid line) and 2344 GMT (dashed. . 68
31. Moisture convergence at 2130 GMT (solid line) and 2344 GMT (dashed . . 69
32. Relative vorticity at 2130 GMT (solid line) and 2344 GMT (dashed . . . 70
33. Surface and 500 mb synoptic maps at 1200 GMT on 30 July 1981, with . . 72
34. Specific humidity, relative humidity, and total specific atmospheric . 73
35. Kinematic convergence, moisture convergence, and relative vorticity. . 74
36. Specific humidity at 1830 GMT (solid line), 2340 GMT (long dashed. . . 76
37. Total specific atmospheric energy at 1830 GMT (solid line), 2340 GMT . 77
38. Kinematic convergence at 1830 GMT (solid line), 2340 GMT (long 78
39. Moisture convergence at 1830 GMT (solid line), 2340 GMT (long dashed . 79
40. Relative vorticity at 1830 GMT (solid line), 2340 GMT (long dashed . . 80

ABSTRACT

Rawinsonde data collected during the Cooperative Convective Precipitation Experiment (CCOPE) were analyzed to search for evidence of surface/upper-air coupling in southeastern Montana. CCOPE, an outgrowth of the HIPLEX-I weather modification project, was conducted near the semi-arid region of Miles City, Montana, during the summer of 1981. Five rawinsonde stations were used in a limited station analysis scheme to examine three periods possessing varying degrees of convection.

The case-studies covered a severe-storm period (June 12-13), which produced radar reflectivities in excess of 50 dBz and a relatively large amount of precipitation; an intermediate convective period (June 20-21) characterized by the occurrence of small, semi-isolated cumuli selected as experimental units for the HIPLEX-I weather modification experiment; and a convectively benign period (July 30-31) with little or no visible convection. Surface/upper-air coupling during these periods was investigated by comparing vertical plots of areally averaged primary and derived meteorological parameters with corresponding temporal surface patterns.

Results suggest that surface/upper-air coupling, manifest as downward-propagating sinusoidal convergence and vorticity patterns, is more clearly established during the severe-storm period, evident to a lesser degree during the intermediate convective period, and absent during the benign period. Analogous analyses using nearby surface stations indicate that these patterns are reflected on the surface. However, the strongest evidence of surface/upper-air coupling based on surface information alone appears to be surface convergence and relative vorticity couplets of like sign.

Other features of the severe-storm period include a low-level jet with significant moisture advection, and an unstable total specific atmospheric energy profile aloft. These features were less striking or absent on the other case-study days.

CHAPTER 1

INTRODUCTION

Upper-Air Measurements

The atmosphere aloft is routinely sampled by instrumented balloons called rawinsondes. These balloons are released at the surface and transmit the pressure, temperature, and humidity of the air through which the instrument is ascending. In addition, the wind speed and wind direction of the upper atmosphere are derived from balloon positions obtained by tracking the balloon from its release point to its position at the time the balloon bursts. When synoptic data from three or more proximate soundings are combined, estimates of other meteorological parameters are possible; e.g., the horizontal velocity divergence, the horizontal moisture convergence, the vertical component of the vorticity, and the vertical component of the wind.

The National Weather Service (NWS) schedules two soundings per day at 0000 and 1200 GMT (Greenwich Mean Time) from approximately 80 sites in the contiguous United States. The NWS sounding network is sufficient for identifying the migratory high and low pressure systems prevalent over the continental United States. However, it is inadequate for forecasting gross processes associated with even the larger convective events, such as those associated with squall lines (House, 1960), which have a characteristic length on the order of 10^4 - 10^5 m (Holton, 1972).

The ability of the synoptic-scale soundings to measure smaller convective events, such as an isolated thunderstorm having a characteristic length of from

1-50 km (Matthews, 1983), is even more limited. Yet the study of such mesoscale phenomena has been selected as a national objective for the atmospheric sciences by the National Academy of Sciences (1980); with a high priority on the identification of the mechanisms which trigger and sustain severe convective storms.

In order to investigate the upper-air environment affected by mesoscale convective complexes, a rawinsonde network that samples at the length and time scales of the event itself is required. Using Orlanski's (1975) scheme for classifying subsynoptic scale phenomena :

meso α : 200 - 2000 km, 6 - 36 h

meso β : 20 - 200 km, 1 - 6 h

meso γ : 2.0 - 20 km, 0.1 - 1 h

a rawinsonde network that would adequately measure isolated convective phenomena would require a network spacing in the meso γ - meso β scale.

The Cooperative Convective Precipitation Experiment

Just such a rawinsonde network was established within a surface mesoscale network (mesonet) for the Cooperative Convective Precipitation Experiment (CCOPE), conducted in the semi-arid region east of Miles City, Montana during the summer of 1981. CCOPE was a cooperative venture funded primarily by the U.S. Bureau of Reclamation (BUREC) and the Convective Storms Division (CSD) of the National Center for Atmospheric Research (NCAR). Other federal agencies, universities, and private organizations, as well as personnel from five different countries participated (BUREC, 1982). CCOPE was designed to evaluate "the potential of convective cloud modification techniques and [to predict] convective precipitation and associated severe weather" (Dennis, et al.,

1984). The CCOPE project was initiated because the resources available to the High Plains Experiment (HIPLEX) were insufficient to adequately resolve questions about the physical processes attendant with convective events.

HIPLEX, which itself was essentially a continuation of the BUREC's Project Skywater experiment, was implemented "to reduce the scientific uncertainties concerning both natural and artificially modified precipitation processes in warm season convective clouds of the High Plains region of the United States" (Smith, et al., 1984). The experimental design of HIPLEX embodied three phases: an exploratory study, experiments on single clouds and cloud systems, and an area experiment.

The exploratory phase of HIPLEX was conducted in Montana, Kansas, and Texas in the mid-1970s. By early 1979, the HIPLEX scientists had obtained enough information to develop a specific experimental plan for Phase 2; i.e., the randomized seeding of small, semi-isolated, cumulus congestus clouds. HIPLEX-I, the initial part of Phase 2, was conducted during the summers of 1979 and 1980. The number of test cases occurring during these two summers was less than had been climatologically expected and, rather than extend HIPLEX-I, the decision was made to conduct CCOPE.

The resulting cooperative effort established the largest mesonet in the world: 123 surface stations covering 22400 square kilometers. In addition, 14 aircraft, up to 8 rawinsonde units, 1 BUREC Skywater radar, and a network of 7 other radars having Doppler capability were operated during CCOPE (BUREC, 1982). The information derived from this massive data gathering network would have contributed to subsequent phases of the HIPLEX project; however, funding for HIPLEX was terminated in 1981.

Focus of Current Study

The cessation of HIPLEX before analysis of the CCOPE data was completed left many of the fundamental questions about convective processes unanswered. Rather than relegate the CCOPE database to the archives, however, funds were solicited from the National Science Foundation to examine triggering mechanisms and other meteorological features which would influence the development and sustenance of convective complexes (Heimbach and Engel, 1981). A convective complex was defined to be a "radar echo that exceeded 30 dBz and reached an altitude of 9 km MSL [Mean Sea Level] or higher during its lifetime, but not necessarily simultaneously" (Heimbach and Super, 1980).

One of the primary unresolved problems addressed in the proposal was the identification of successful predictor-covariates of convection. The number of potential candidates was impressive. For example, Acherman, et al. (1976) selected 47 promising candidates from a list of 199 in their summary of the design for Phase 2 of HIPLEX. Heimbach and Engel (1981), however, selected 18 covariate candidates for the statistical part of their study. These were organized into two groups: those found reasonably successful in previous studies, such as surface kinematic and moisture convergence, vorticity, and mixing ratio; and a set of newly proposed covariates including latent energy and convective destabilization.

The fundamental assumption underlying the statistical analysis is that the surface boundary layer is coupled to convective events aloft. The assumption of coupling provides the physical link that allows a causal explanation to be applied to the correlation. Therefore, the conditions under which this assumption is valid need to be defined.

Thesis Statement

The purpose of this study is to examine the CCOPE rawinsonde database for evidence of surface/upper-air coupling. Specifically, the hypothesis is advanced that surface mesoscale features commonly associated with convection are coupled to convective phenomena aloft in southeastern Montana. The conditions under which surface/upper-air coupling occurs is determined by investigating three periods possessing different degrees of convection. The case-studies consist of a severe-storm period (June 12-13) producing radar reflectivities in excess of 50 dBz with a large quantity of precipitation; a intermediate convective period (June 20-21) possessing the small, semi-isolated cumulus congestus clouds selected as experimental units for the HIPLEX-I project; and a convectively benign period (July 30-31) with little or no visible convection.

CHAPTER 2

HISTORICAL BACKGROUND

The Thunderstorm Project

The Thunderstorm Project, summarized in a notable and enduring study by Byers and Braham (1949), arose out of a need to better understand the extreme hazard that these convective events posed to aircraft, especially since pilots could no longer restrict their flights to good weather. The fortuitous close of the war allowed the conversion of wartime equipment and personnel to peacetime research, and enabled the study to be conducted on a more complete scale than at any prior time.

The Thunderstorm Project studied thunderstorms occurring mostly in maritime-tropical air masses near Orlando, Florida and Wilmington Ohio. A major feature identified during the study was "convection units having similar properties and characteristics" (Byers and Braham, 1949) localized within the thunderstorm. These regions were defined as "cells". The lifetime of thunderstorm cells could exceed 30 minutes, during which time they tended to retain their identity and move with the body of the storm.

Three stages characterized the life of a thunderstorm cell : the cumulus stage, dominated by an updraft throughout the cell; the mature stage, in which a downdraft is initiated in part of the cell by viscous drag from falling water droplets, and subsequently enhanced by the entrainment of the colder ambient air surrounding the cell; and the dissipating stage, in which the downdraft, growing at the expense of the updraft, eventually cuts the updraft off from its

source region. With the dissipation of the updraft and subsequent removal of the source of rainfall, the cell eventually dies.

Those surface features attending the life cycle of the thunderstorm cell were also described. The cumulus stage, which normally lasted from 10 to 15 minutes, was accompanied by a slightly lowered surface pressure, and horizontal velocity convergence up to 1/2 h prior to the first radar echo. This surface convergence accounts for the "calm before the storm" in cases where the inflow opposes the prevailing winds.

By the time the cell develops into the mature stage, the cold-core downdraft carrying the rain reaches the surface, and flows outward from the rainfall area. The wind speed in the downstream portion of the cold air dome usually far exceeds the wind speed in the upstream portion, becoming an asymmetrical "gust-front" which travels ahead of and in the direction of the storm itself. This gust-front or "micro-cold front" (Byers and Braham, 1949) is accompanied by strong horizontal velocity divergence, a sudden surface temperature drop, and a sharp pressure rise. The heaviest rainfall was found to occur within the area of the maximum horizontal velocity divergence, but somewhat earlier due to the greater velocity of the water droplets with respect to the downdraft. The mature stage usually lasts for 15 to 30 minutes.

During the dissipating stage the precipitation gradually ceases, the surface pressure recovers from the sharp pressure jump, and the horizontal velocity divergence diminishes. The dissipating stage lasts for approximately 30 minutes.

Not all thunderstorm cells follow this pattern. For example, vertical wind shear may cause the downdraft region to occur outside of the initial cell, and thus prolong the life of the updraft. In fact, the cell may dissipate without

establishing the downdraft evident during the normal dissipating stage. On the other hand, some cumuli fail to develop into thunderstorms. Byers and Braham (1949) surmised that return settling of the environment around large thunderstorm cells may inhibit development of nearby clouds. Return settling refers to large-scale downward air motion compensating the localized updraft regions in developing cumuli.

Kinematic analysis of balloon ascents into isolated clouds revealed an interesting pattern of alternating convergence/divergence regimes aloft during ten of the seventeen soundings taken. Each of these storms had developed a downdraft with rain and showed low-level divergence under a layer of convergence, with divergence again above about 6 km. The low level divergence was a result of the downdraft, while the convergence aloft resulted from horizontal inflow of the ambient air through the cloud boundary. In the remaining seven balloon ascents, the rain had not begun at the surface, and the profiles showed convergence at all levels.

Relevant Surface Research

Noting that Byer and Braham's (1949) observation of the occurrence of surface convergence 20-30 min before the appearance of the first radar echo had received little attention since initially reported, Ulanski and Garstang (1978) studied the role that surface conditions, primarily the horizontal wind speed and direction, played in the life cycle of convective storms. The premise was that a time-persistent cellular pattern existed in the surface divergence and vorticity fields, and that these fields were correlated to convective events. Using data from the surface mesonet established during the Florida Area Cumulus Experiment (FACE) in 1971 and 1973 (see Woodley and Sax, 1976), objectively

analyzed maps of surface divergence and vorticity were obtained for 5-min intervals.

A direct relationship between total storm rainfall and the areal extent of the surface convergence was found. The size of the surface area of convergence was observed to be a critical factor in controlling the total amount of rainfall produced by a given convective storm. This is because the size of the surface convergence area determines the amount of moisture supplied to the storm. For intense convective events, the larger portion of surface moisture is supplied during the storm's mature stage.

The size of the initial convergence cell was also related to the point maximum rainfall. The size of the convergence cell was parameterized by defining a "spatial index" as "the shortest distance (km) from the center of the convergence cell to the zero isopleth of divergence. . . computed as an average distance over the first 15 min of the life of a center of convergence" (Woodley and Sax, 1976). A linear correlation coefficient of 0.72 was found between the spatial index and point rainfall.

A direct relationship was discovered between the storm maximum point rainfall and the length of time that surface convergence existed before the rain. Because of the lead time, which exceeded 90 min in the larger storms studied, it was concluded that the surface convergence caused the convective storm, and was not a result of it. Though not specifically mentioned as such, surface/upper-air coupling is suggested by the observation that "in each case the shower developed in the vicinity of the initial convergence cell" (Woodley and Sax, 1976). It was also observed that the initial field of positive convergence and vorticity changed to negative values during the time of maximum rainfall.

Relevant Upper-Air Research

Prior to HIPLEX, weather modification experiments did not recognize the need for mesoscale rawinsonde observations (Matthews, 1983). A significant study of a mesoscale rawinsonde network was, however, accomplished by Fankhauser (1969). He applied objective analysis techniques to a 9-station network in Oklahoma to "appraise the sounding system's limitations and reliability for resolving the mesoscale circulations associated with convective processes." The primary deficiencies identified in the rawinsonde system were the inherent temporal and spatial limitations in the sampling network, and assumed measurement and analysis errors. These errors included non-simultaneous release times, balloon drift, varying ascent rates, decreasing wind measurement accuracy with decreasing elevation angles (increasing height), and error accumulation with height due to vertical integration of the continuity equation (see Chapter 5). The effects of these deficiencies were minimized by spatial and temporal smoothing of the data reduction and analyses, using both objective and subjective techniques. However, the smoothing techniques and basic observational limitations did not allow downward extension to scales on the order of singular thunderstorm processes. Nevertheless, it was found that good qualitative agreement existed between the kinematic divergence and vertical motion, and thunderstorm location and intensity.

During the summer of 1976, a 5-station rawinsonde network was operated at the Texas HIPLEX site. Scoggins, et al. (1978) reported that moisture convergence, vertical motion, and vertical moisture flux proved to be good covariates of convection, though nearly all of the surface and upper-air variables showed some response to convective activity.

Relevant Research in Southeastern Montana

The foregoing studies were all accomplished outside the Montana High Plains. Doneaud, et al. (1983) performed a case-study analysis on the 1980 HIPLEX surface mesonet data collected in southeastern Montana to investigate the surface kinematic fields attendant with convective storms. It was found that convergence cell development preceded radar echoes and rain, in agreement with earlier studies. An interesting feature of the convective clouds in southeastern Montana was that they received a greater moisture inflow and, thus, produced less rain efficiency than clouds with similar rainfall duration and amounts in humid climates.

CHAPTER 3

DATABASE DESCRIPTION

The CCOPE surface mesonet consisted of 96 BUREC PROBE (Portable Remote Observation of the Environment) stations, operated by the Montana Department of Natural Resources and Conservation, and 27 NCAR PAM (Portable Automated Mesonet) stations. Seventy-one of the PROBE stations were placed in a 9 X 8 square grid, with a station-to-station spacing of approximately 20 km. The remaining PROBE and all the PAM stations were established in a dense, irregular inner network under Doppler cover, with a station separation of approximately 7 km (see Fig. 1).

The BUREC PROBE stations transmitted hourly blocks of 5-min arithmetically averaged temperature, pressure, relative humidity, east and north wind components, and cumulative precipitation to the GOES-West (Geostationary Observational Earth Satellite). The information was then retransmitted to the Denver BUREC downlink, and to a backup site at NOAA-NESS in Wallops Island, Virginia (BUREC, 1982).

The NCAR PAM stations telemetered 1-min average dry-bulb temperature, wet-bulb temperature, pressure, east and north wind components, peak wind velocity during each minute, and the rainfall to the PAM base at the Miles City airport.

The supporting rawinsonde network consisted of 5 primary stations (see Table 1) operated by Texas A&M University (TAMU), a redundant system at Miles City operated by Western Weather Consultants, Inc. (WWCI), and 2 stations operated in late June and early July by the Alberta Research Council.

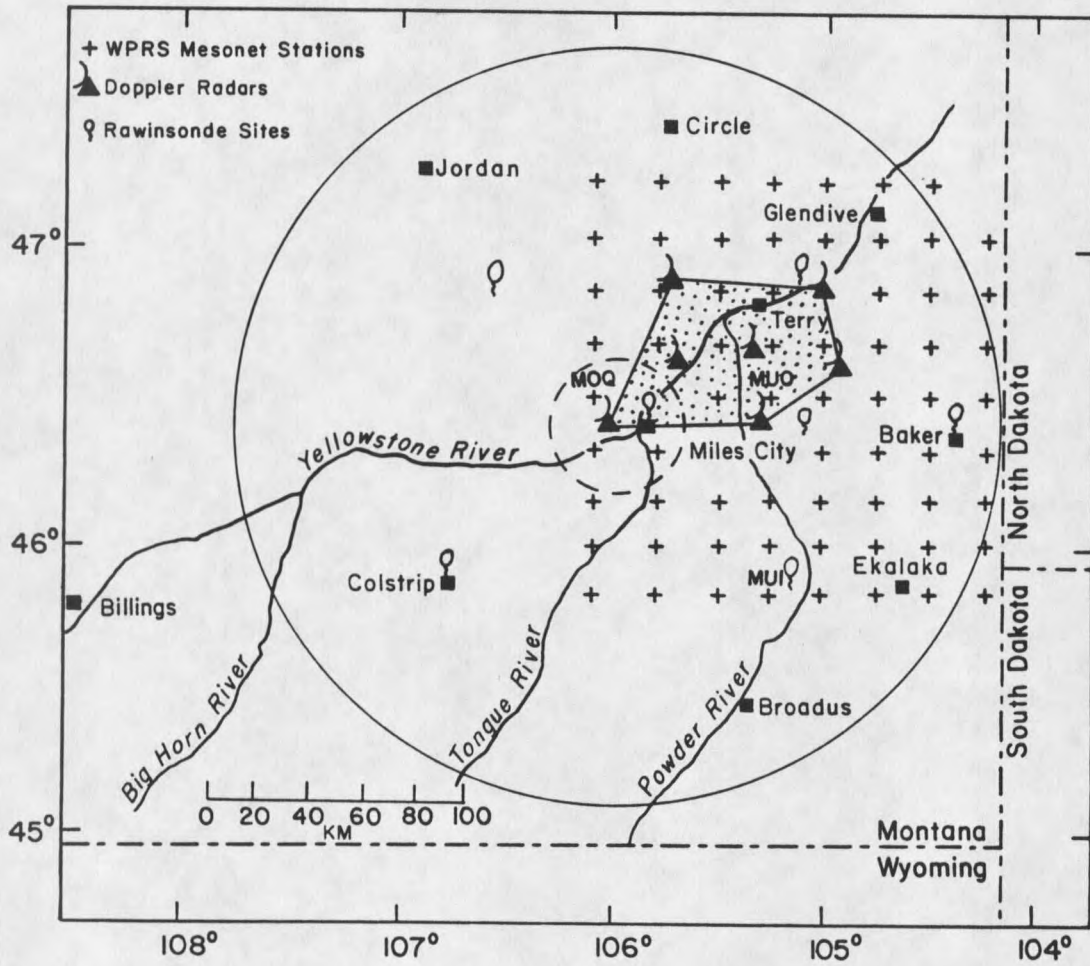


Figure 1. CCOPE surface mesonet, radar, and rawinsonde sites.

Table 1. The location and elevation of the CCOPE rawinsonde sites (BUREC, 1982)

Station	Elevation in meters	Latitude (N)			Longitude (W)		
		Deg	Min	Sec	Deg	Min	Sec
Baker	903	46	21	10.6	104	13	26.3
Glendive	803	47	05	00.0	105	06	42.6
Knowlton	954	46	20	13.8	105	04	40.0
Miles City	800	46	26	05.5	105	52	30.0
Powderville	866	45	45	20.3	105	06	07.0

TAMU took soundings on 54 days during 21 May to 6 August; usually at a frequency of one sounding every 1.5 h between 1800-0300 GMT (1200-2100 MDT [Mountain Daylight Time]), while WWCI took 2 soundings daily, 6 days a week on a non-rigid schedule consisting of one early in the morning (1145 GMT) and one in the early afternoon at 1930 GMT. The sounding data consisted of the temperature and relative humidity ordinates, the pressure, time after release for each pressure contact, and the azimuth and elevation angles at 30-second intervals. Normally, soundings were terminated at 100 mb, which is approximately 16 km.

The rawinsonde data selected for this study were collected by NCAR, who also performed the necessary data integrity tests and post-screening procedures. Wind information contained in this dataset had been lightly smoothed with a nine-point filter¹ and were interpolated to pressure-contact times where necessary. No additional screening or editing of these data were accomplished, other than simple spot-checks on the database using a hand calculator and the raw data contained on microfiche.

¹Weights were 0.3200156553, 0.2643210644, 0.1343767864, 0.0114831529, -0.0458900942, -0.0377520979, -0.0064753717, 0.0111929411, 0.0087357913

Radar information was used to assist in the identification of the case-study periods selected for this study. These data came from the BUREC 5.4 cm Skywater radar which was located about 3 km west of Miles City. The radar beam width was 1 deg, and scans were made from elevation angles 1 - 12 deg. Under normal operation, the radar scans were taken every 5 min; however, a rapid-scan mode was also available, which scanned every 3 min. These data were processed by the BUREC staff at Miles City (Heimbach and Engel, 1986).

CHAPTER 4

PROCEDURES

Sequence of Operations

The underlying premise for this study was that surface/upper-air coupling could be identified if vertical profiles of those parameters commonly associated with convective activity were generated. The features manifest in the vertical profiles would be evident at the surface as well, if coupling had been established. Thus, though the study would focus on the rawinsonde data, the surface database would have to be accessed as well.

The initial step was to inspect the CCOPE surface data for obvious errors and correct them. This was accomplished by referring to field notes and visually inspecting each day's data, which were available in graphical form. The types of errors observed during the visual inspection included transmission noise and obvious errors in the parameter traces. Two researchers independently reviewed each day's data to minimize oversights and personal bias. The necessary corrections were then entered into a recalibration file, which could be accessed when the surface data were processed. The recalibration file contained other corrections to the surface database which were not readily evident on the parameter traces, such as pressure recalibration factors from NCAR.

It was also presumed that the vertical profiles would vary according to the degree of convection. For example, Ulanski and Garstang (1978) observed that divergence values discriminated between convectively active and inactive

periods. Accordingly, it would be expected that the kinematic values aloft would show similar discrimination. Therefore, the vertical profiles would have to cover periods possessing different degrees of convection in order to determine the extent that surface/upper-air coupling depended on the magnitude of the convection. To this end, operational field notes and radar data were examined to select three case-study periods with high, intermediate, and low degrees of convection.

June 12-13 was selected to represent the period with high convective activity; i.e., the "severe-storm" period. During this period, a large convective complex traversed the mesonet, producing large amounts of precipitation with probable hail. In addition, a tornado watch had been issued for the area south of Miles City. For the intermediate, or "HIPLEX-I" period, June 20-21 was selected because it contained the isolated cumulus congestus clouds sought as experimental units during the HIPLEX-I weather modification experiment. A cloud-free period, July 30-31, was selected for the low, or "benign" period. The terms "severe-storm", "HIPLEX-I", and "benign" will be used in the remainder of this paper to reference the case-study periods.

Next, the rawinsonde data were obtained on magnetic tape from the BUREC, who had the responsibility of archiving all the CCOPE data. Procedures for downloading and accessing the rawinsonde data on an IBM PC were developed (see Fig. 2). Several man-weeks were spent developing algorithms that would both analyze the raw rawinsonde data and interface with existing (surface) software. After the BUREC datatape arrived, the rawinsonde program's processing schemes were tested against NCAR microfiche data. A discrepancy was discovered between the BUREC processed data and the NCAR microfiche data, even though the raw data values for the two datasets were similar.

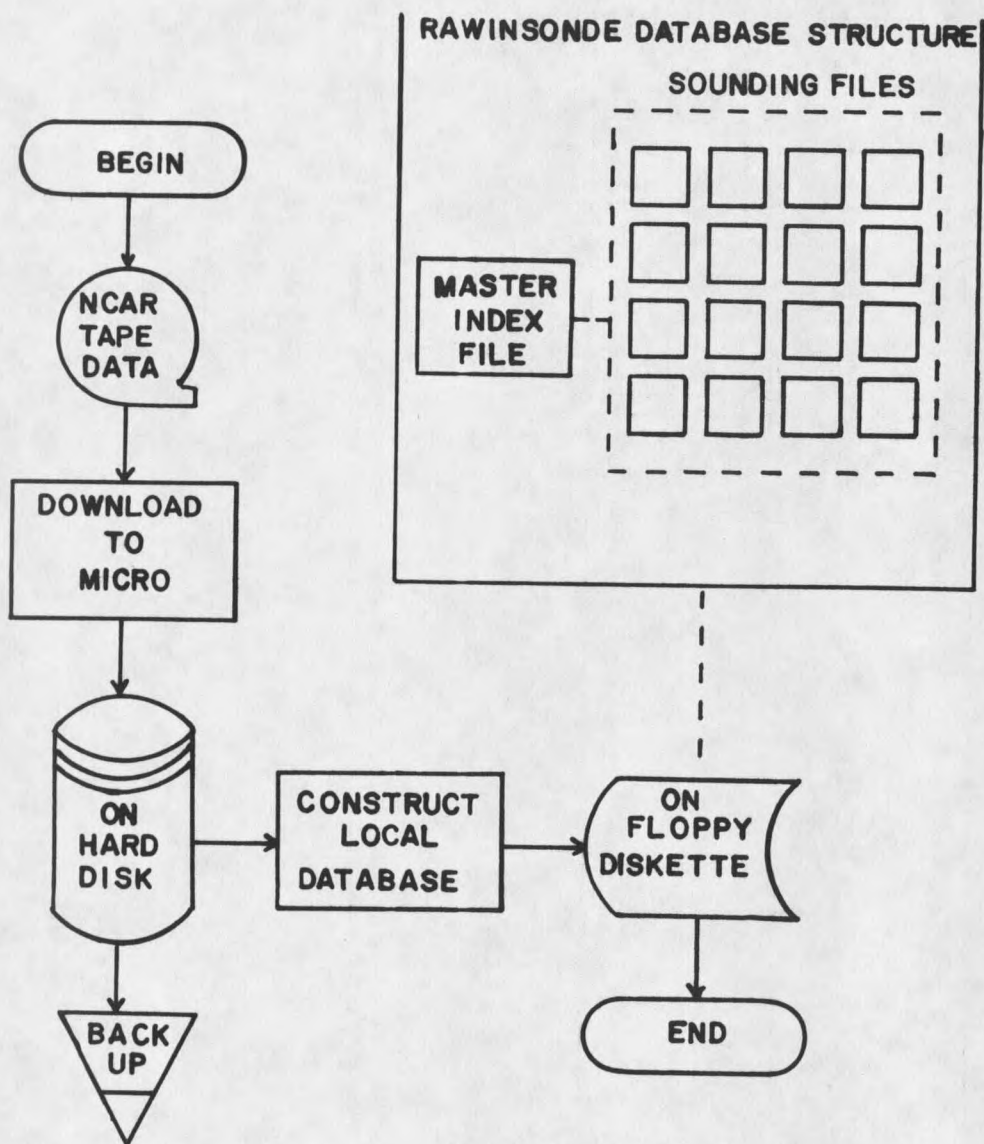


Figure 2. Procedures for construction of the rawinsonde database on the IBM PC.

Following procedures outlined by Retallack (1971), several hand calculations were performed on both datasets. It was discovered that an error existed in the BUREC data, which was eventually traced to an initialization error in BUREC's RAOB program. Rather than wait for BUREC to correct the error and generate a new datatape, rawinsonde data were obtained from NCAR. Fortunately, the NCAR data formats proved to be more suitable for the types of analyses performed in this study.

After new algorithms were written to process the NCAR database, and the database was downloaded to diskette, a series of preliminary profiles were generated. These revealed that the kinematic patterns were more coherent in the lower 7 km than above this level. Since winds in the 900 mb (1km) to 400 mb (7km) range are the most reliable, and the kinematically derived vertical velocity does not require the corrections specified by O'Brien (1970) in this region (Matthews, 1983), vertical profiles were restricted to the lower 7 km.

Most of the investigations were further narrowed to one quadrant of the rawinsonde network, because similar profiles were apparent in all quadrants. The southwest quadrant, bounded by Knowlton, Miles City, and Powderville (see Fig. 1), was selected because the first convective complex affecting the severe-storm period entered the mesonet from the southwest.

Data Adjustments

Interpolation

Rawinsonde data for specific times between soundings were synthesized using linear interpolation to account for varying sounding release times and differing balloon ascent rates, as in Fankhauser (1969). The interpolation scheme also provided a means to supply estimates for missing data. Using the

criteria outlined in Fuelberg and Printy (1983), interpolation for missing data was used only if the time interval between rawinsondes was less than 6 h, and the target time fell between the first and last observation times, thus avoiding extrapolation. Logarithmic interpolation between pressure levels was used when parameters were required for levels not corresponding to contact times.

Balloon Drift

In order to determine the degree that balloon drift affected the calculated kinematic values, divergence was calculated for the northwest and northeast quadrants of the rawinsonde network, with and without balloon drift (see Table 2). Since the values differed by less than ten percent in both cases, it was decided to ignore balloon drift in the algorithms.

Table 2. Divergence calculations with and without balloon drift at the 150 mb level on June 20, 1981 at 2200 GMT.

Quadrant	Divergence Values	
	Without Balloon Drift	With Balloon Drift
Northwest	$-3.82 \times 10^{-5} \text{ s}^{-1}$	$-3.50 \times 10^{-5} \text{ s}^{-1}$
Northeast	$-2.21 \times 10^{-4} \text{ s}^{-1}$	$-2.45 \times 10^{-4} \text{ s}^{-1}$

Surface/Upper-Air Comparisons

Network Differences

One of the factors affecting a network's ability to detect an atmospheric event is the observational sampling density. With a sampling distance of s , the minimum resolvable scale length is $2s$. This is analogous to the Nyquist frequency, which specifies that at a sampling period of T , the smallest period

that can be sampled is $2T$. Unfortunately, the possibility of interfering radio signals limits the spacing of the rawinsonde network to about 55 km (Fankhauser, 1969). The CCOPE rawinsonde spacing varied from about 60 to 85 km. The smallest event that could be sampled by the rawinsonde network, then, would have a scale length approximately three or four times that measurable by the surface network. This would seem to preclude a direct comparison between the two sampling networks (see Achtemeier, 1980). However, this problem was circumvented by using a limited set of surface stations, selected on the basis of their geographical locations relative to the rawinsonde release sites, in the comparison (MOQ, MUO, MUI in Fig. 1). Accordingly, the limited-station analysis (LSA) procedures developed by Heimbach and Engel (1986) for analyzing the CCOPE surface data were adapted for use with the rawinsonde data.

Coordinate Reference Frames

Surface parameters calculated by the LSA algorithms are based in a constant-altitude (AGL [Average Ground Level]) coordinate system. Therefore, the surface kinematic calculations fail to account for additional terms, i.e., wind shear and terrain slope, that appear in a non-horizontal reference frame (Schaefer, 1973). The rawinsonde calculations, however, are based in a constant-geopotential height above mean sea level (MSL) coordinate system. The analyses needed to allow for a comparison between the rawinsonde "surface" calculations, which would be at the horizontal level of the highest surface station, and the surface mesonet sites. To accomplish this, the rawinsonde programs calculated N "surface" parameters, where N is the number of stations at unique elevations. These calculations were "stepped-up" until the first possible horizontal level was attained. Thereafter, the parameters were

calculated at horizontal levels. The difference between the surface and first horizontal level, then, provided a measure of the effect of wind shear and terrain slope. Terrain-induced lifting, however, was not directly considered by the rawinsonde programs.

Data Processing Methods

All data processing was accomplished on an IBM PC, since the estimated costs to perform the analyses on a mainframe were prohibitive. Specialized software were developed for this study; however, a complete description of the programming procedures is beyond the scope of this paper. Therefore, documentation is limited to program listings, which are provided in the appendices. The PLOT-10 emulation software, used to generate the plots on a dot-matrix printer, is copyrighted and, therefore, not included.

Evaluation of Meteorological Parameters

The methods used by the LSA procedures to evaluate the meteorological parameters for the rawinsonde database are detailed below. Unless otherwise noted, the formulae follow Saucier (1972).

Vapor Pressure

The saturation vapor pressure, e_s , was calculated using the semi-empirical quadratic formulation given by Tabata (1973) :

$$\log e_s = 8.42926609 - 1.82717843(10^3/T) - 0.071208271(10^3/T)^2, \quad (1)$$

where e_s is in millibars, and T is the absolute temperature in degrees Kelvin. The ambient vapor pressure, e, may be found by substituting the dewpoint temperature, T_d , for the ambient temperature in Eq. 1.

Absolute Humidity

The absolute humidity, or density of water vapor, ρ_w , is found using the equation of state :

$$\rho_w = m_w e / R^* T, \quad (2)$$

where m_w is the molecular weight of water (18 g/mol) and R^* is the universal gas constant (8.316963×10^7 erg/mol-deg).

Specific Humidity

The specific humidity, q , is the mass of water vapor per unit mass of the moist air mixture. The total density, ρ , of the air is the sum of the dry-air and the absolute humidity:

$$\rho = \rho_d + \rho_w = m_d(p - 0.37803e) / R^* T, \quad (3)$$

where m_d is the molecular weight of dry air (28.966 g/mol) and p is the ambient pressure in millibars. Thus, the specific humidity is given by :

$$q = \rho_w / \rho = 0.62197e / (p - 0.37803e). \quad (4)$$

Mixing Ratio

The mixing ratio, r , is the mass of water vapor per unit mass of the dry air with which it is mixed :

$$r = \rho_w / \rho_d = 0.62197e / (p - e). \quad (5)$$

Relative Humidity

The relative humidity, U , is the ratio of the actual to saturation mixing ratio at the same temperature and pressure, expressed as a percent :

$$U = (r/r_s) \times 100\%, \quad (6)$$

where r_s is the saturation mixing ratio.

Virtual Temperature

The virtual temperature, T^* , is the temperature of dry air having the same pressure and density of the moist air :

$$T^* = T(1 + 0.61r). \quad (7)$$

Potential Temperature

The potential temperature, θ , is the temperature of a parcel of air brought dry adiabatically to the 1000 mb level:

$$\theta = T(1000/p)^{(R_d/c_p)}, \quad (8)$$

where c_p is the specific heat of dry air at constant pressure (1.004×10^7 erg/g-deg), and R_d is the ideal gas constant for dry air (0.2870×10^7 erg/g-deg). The ratio R_d/c_p is 2/7 for dry air.

Equivalent Temperature

The equivalent temperature, T_E , is the temperature that a parcel of air would have if it were brought pseudo-adiabatically to the point where all latent heat is realized, and then returned dry-adiabatically to its original partial pressure (Rossby definition) :

$$T_E = T_e^{(Lr/c_p T)}, \quad (9)$$

where L is the latent heat of vaporization, 597.3 cal/g at 273 K.

Equivalent Potential Temperature

The equivalent potential temperature, θ_E , is the dry-adiabatic reduction of the equivalent temperature to the 1000 mb level:

$$\theta_E = T_E(1000/p)^{(2/7)}. \quad (10)$$

Total specific atmospheric energy

The total specific atmospheric energy, E_T , was determined using Darkow's (1968) formula, reduced to units of cal/g-s :

$$E_T = c_p T + gZ + Lq + V^2/2, \quad (11)$$

where Z is the MSL elevation. E_T essentially represents the "static" energy, since the kinetic energy term, $V^2/2$ is negligible.

Horizontal Kinematic Convergence

The horizontal kinematic convergence is the negative of the horizontal divergence of the velocity vector, and may be physically represented as the fractional areal expansion per unit time:

$$\text{Conv}_H = -\text{Div}_H = \vec{\nabla}_H \cdot \vec{V} \approx (1/A)(\Delta A/\Delta t). \quad (12)$$

The initial area bounded by the stations is A , and ΔA is the change in area due to the wind during the time interval Δt . The horizontal convergence was calculated using a special case of the line integral method which was analogous to the Bellamy (1948) technique. Details concerning the adaptation of the technique to computer processing are outlined in Heimbach and Engel (1986).

Vertical Component of the Relative Vorticity Vector

The vertical component of the relative vorticity vector (hereafter simply the relative vorticity) is $\vec{\nabla}_H \times \vec{V}_H$. This is equal to the divergence of the wind transformed by rotating the wind field clockwise 90 degrees:

$$\begin{aligned} u' &= v, \\ v' &= -u, \end{aligned} \quad (13)$$

where $()'$ indicates the transformed wind field.

Horizontal Moisture Convergence

The horizontal moisture convergence is estimated by multiplying the average absolute humidity, ρ , for the area by the horizontal kinematic convergence (Heimbach and Engel, 1986):

$$M_{con_H} = \rho_w \text{Conv}_H. \quad (14)$$

Vertical Velocity

The vertical velocity, w , is found by using the equation of mass continuity (see, e.g., Hess, 1959) :

$$\rho \nabla \cdot \mathbf{V} = 0, \quad (15)$$

and assuming an incompressible atmosphere ($d\rho = 0$) :

$$w = \int_0^H \text{Conv}_H \, dZ. \quad (16)$$

H is the elevation (MSL). The surface boundary condition has $w = 0$, as in Doneaud (1983). In the LSA programs, the vertical velocity was found by summing individual contributions :

$$w_N = \sum_{i=1}^N (1/2)(\text{Conv}_{H_{i-1}} + \text{Conv}_{H_i})(\Delta h) \quad (17)$$

where Δh is the change in height between selected levels.

CHAPTER 5

CASE-STUDY ANALYSES

The southwest quadrant of the rawinsonde network (bounded by Knowlton, Miles City, and Powderville) was the nearest to an approaching convective complex at the start of the severe-storm period (June 12-13). Therefore, it was selected as the primary quadrant for analysis. However, the center station in the rawinsonde network (Knowlton) had only one usable sounding during the HIPLEX-I period. As a result, the southern half of the network (bounded by Baker, Miles City, and Powderville) was selected for study during this period.

Knowlton lies on an approximately east-west line between Baker and Miles City, and is thus properly on the southern half boundary. Therefore, Knowlton should be included as a boundary station when the southern half is analyzed. Heimbach and Engel (1986), however, found that increasing the number of stations around the periphery of the area had little effect on the LSA calculations for the surface stations. This result appears to hold true for the upper-atmosphere as well. Figure 3 compares the horizontal convergence values at 2340 GMT on 12 June for the southern half of the rawinsonde network both with and without Knowlton. The differences are at the noise level. Similar results were observed for the other parameters tested.

The lack of sounding data at Knowlton during the HIPLEX-I period may also affect comparisons between the southwest surface quadrant and the upper-air, as well as comparisons among the case-study periods. However, Heimbach and Engel (1986) found that the responses of the derived parameters became smoother as

